

DTIC F... COPY

(2)

AD-A217 663

Gas Turbine Laboratory
Department of Aeronautics and Astronautics
Massachusetts Institute of Technology
Cambridge, MA 02139

FINAL SUMMARY REPORT

on Contract N00014-81-K-0024

entitled

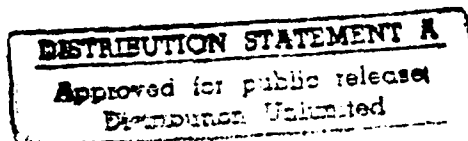
EXPERIMENTAL AND THEORETICAL INVESTIGATIONS
OF FLOWFIELDS AND HEAT TRANSFER
IN MODERN GAS TURBINES

DTIC
ELECTE
JAN 25 1990
S D D

submitted to

Office of Naval Research
Mechanics Division
800 North Quincy St.
Arlington, VA 22217-5000

ATTN: Dr. Gabriel Roy



PERIOD OF
INVESTIGATION:

January 1, 1981 - March 31, 1987

January 1990

90 01 23 224

REPORT DOCUMENTATION PAGE

1a. REPORT SECURITY CLASSIFICATION None			1b. RESTRICTIVE MARKINGS		
2a. SECURITY CLASSIFICATION AUTHORITY			3. DISTRIBUTION / AVAILABILITY OF REPORT		
2b. DECLASSIFICATION / DOWNGRADING SCHEDULE					
4. PERFORMING ORGANIZATION REPORT NUMBER(S)			5. MONITORING ORGANIZATION REPORT NUMBER(S)		
6a. NAME OF PERFORMING ORGANIZATION Massachusetts Inst. of Tech.		6b. OFFICE SYMBOL (if applicable) 31-266		7a. NAME OF MONITORING ORGANIZATION see #8	
6c. ADDRESS (City, State, and ZIP Code) 77 Massachusetts Ave. Cambridge, MA 02139		7b. ADDRESS (City, State, and ZIP Code) see #8			
8a. NAME OF FUNDING / SPONSORING ORGANIZATION Office of Naval Research		8b. OFFICE SYMBOL (if applicable)		9. PROCUREMENT INSTRUMENT IDENTIFICATION NUMBER	
8c. ADDRESS (City, State, and ZIP Code) 800 N. Quincy St. Arlington, VA 22217-5000		10. SOURCE OF FUNDING NUMBERS			
		PROGRAM ELEMENT NO.		PROJECT NO.	TASK NO.
				WORK UNIT ACCESSION NO.	
11. TITLE (Include Security Classification) Experimental and Theoretical Investigations of Flowfields and Heat Transfer in Modern Gas Turbines					
12. PERSONAL AUTHOR(S) A.H. Epstein, M.B. Giles, G.R. Guenette, W.T. Thompkins, Jr.					
13a. TYPE OF REPORT Final Summary Report		13b. TIME COVERED FROM 1/1/81 TO 3/31/87		14. DATE OF REPORT (Year, Month, Day) 1/16/90	
				15. PAGE COUNT 33	
16. SUPPLEMENTARY NOTATION					
17. COSATI CODES			18. SUBJECT TERMS (Continue on reverse if necessary and identify by block number) Turbines, Heat Transfer		
FIELD	GROUP	SUB-GROUP			
19. ABSTRACT (Continue on reverse if necessary and identify by block number) Aerodynamics and heat transfer of high pressure turbines were studied computationally and experimentally. Two- and three-dimensional steady, and two-dimensional unsteady viscous codes were written. An 0.3 second duration, full rotating stage, test rig was built and instrumented to yield both steady state and time-resolved data. The CFD solution and experimental data were in good agreement. The rotating rig data resembled that from cascades rather than full scale engines. <i>Keywords: High pressure turbine stages.</i> <i>(ESJ)</i> <i>A</i>					
20. DISTRIBUTION / AVAILABILITY OF ABSTRACT <input type="checkbox"/> UNCLASSIFIED/UNLIMITED <input type="checkbox"/> SAME AS RPT. <input type="checkbox"/> DTIC USERS				21. ABSTRACT SECURITY CLASSIFICATION	
22a. NAME OF RESPONSIBLE INDIVIDUAL Alan H. Epstein				22b. TELEPHONE (Include Area Code) (617) 253-2485	
				22c. OFFICE SYMBOL 31-266	

1.0 EXECUTIVE SUMMARY

This is the final summary report of a multi-year effort to explore the fluid mechanics and heat transfer in high pressure turbine stages. One major motivation was the observation that turbine rotor blade heat transfer is not well predicted by existing analytical or computational techniques, implying that the fundamental flowfield structure is not well understood. The central focus of this work was the development of new experimental and computational tools and the application of those tools to turbine rotor flows.

A new type of short duration turbine test facility was developed, a blowdown turbine. This rig simulates all of the non-dimensional flow parameters known to be important to turbine fluid mechanics and heat transfer for approximately 0.3 sec, sufficient time for flowfield and heat transfer measurements. New types of high frequency response instrumentation was also developed as an integral part of this program. The rig and instrumentation worked quite well and are now being duplicated elsewhere.

Three new CFD codes were developed to aid this research. Two- and three-dimensional Reynolds averaged Navier-Stokes codes were used to examine the time averaged or steady flow in the turbine. A thin shear layer, 2-D, multi-blade row, Reynolds averaged viscous code was written to explore the unsteady flow in the machine. These codes have been distributed to, and have been used at, various government and industrial organizations.

The experimental results show the flow and heat transfer in the turbine to be highly unsteady with blade passing modulations to be on the order of 100% of the mean. The fluctuations may not be characterized as small perturbations. Both the mean level and the fluctuations very closely match those measured in a two-dimensional cascade of the same blade profiles with unsteadiness introduced by upstream bar passing. Thus, the rotating rig data more closely resembles cascade data than engine data, implying that important phenomena were not modelled in the blowdown turbine facility. Turbulence intensity and turbine inlet temperature nonuniformities are the most likely candidates and future work should concentrate here. The CFD solutions closely matched the cascade and rotating rig data and were used to explain the physical significance of various structures observed in the measurements, demonstrating the utility of a joint computational-experimental effort.

2.0 CONTRIBUTORS TO THIS RESEARCH

Faculty and Staff

E.E. Covert*

A.H. Epstein*

M.B. Giles*

G.R. Guenette

R. Haines

R.J. Norton

W.T. Thompkins, Jr.*

C. Yuzhang

Graduate Students

R. Bush

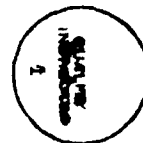
J. Holt

M.J. Lewis

B. Zaretsky

STATEMENT "A" per Dr. Gabriel Roy
ONR
TELECON 1/24/90 CG

Accession For	
NTIS CRA&I	<input checked="" type="checkbox"/>
DTIC TAB	<input type="checkbox"/>
Unannounced	<input type="checkbox"/>
Justification	
By <i>per call</i>	
Description/	
Availability Codes	
Dist	Avail and/or Special
A-1	



* Principal Investigator

3.0 INTRODUCTION

Intense development of high pressure aircraft turbines over the past 40 years has yielded very high temperature machines which can operate for reasonable lifetimes after extensive and expensive refinement. These designs are at least as dependent on this empirical refinement as on advances in the fundamental understanding of heat transfer and fluid mechanics. Turbine design is now characterized by a tremendous variation in *a priori* predictive accuracy for new designs -- from a few percent in some regions to factors of two in others.

The fundamental driver in the design of modern high pressure turbines is the precision to which the turbine metal temperature (and therefore the heat transfer) must be predicted. A 20°F variation in a turbine with a 1000°F gas-metal temperature difference means a factor of two in turbine life. This level of accuracy is now beyond the state of the art for all new designs. The second primary concern is aerodynamic efficiency, especially for transport and long-range engines. Here, increases of efficiency as low as 1/2% are extremely significant.

It was clear that then-existent models of turbine flowfields were inadequate for the job of accurate, reliable predication and analysis of turbine flowfields. Furthermore, this inadequacy appeared to be based upon the incomplete and inaccurate understanding of this exceedingly complex flow. Areas of large uncertainty no longer lay in the traditional concerns of mean line turbine aerothermodynamics (two-dimensional based physics), but rather in those areas of the fluid physics which result from the three-dimensional, rotational, unsteady nature of the high pressure turbine stage, which are not well accounted for in present turbine design systems.

There are two primary effects of rotation: those stemming from the centrifugal and Coriolis forces due to the tangential and radial components of the three-dimensional flowfield, and those stemming from the buoyancy due to the temperature variations introduced by the cooling flow. Unsteady effects in turbines stem from blade row interactions, vortex flows, and tip leakage flows. Of particular concern are the time dependence of the boundary layer on the rotor due to the vane wakes, and the unsteadiness of the casing flow due to blade tip passage. It is to these areas that this program was addressed, with particular attention to effects of the shear layer transport on the

rotor flow and heat transfer. Thus, a combined experimental and computational program was initiated under the joint sponsorship of ONR and Rolls Royce to explore the fluid physics of high pressure turbine stages.

The following is a summary report of the activities of this program, divided into experimental and computational sections. For detailed information, the reader is referred to the technical publications produced under this contract listed at the end.

4.0 EXPERIMENTAL PROGRAM

4.1 Experimental Apparatus

As the performance required of high pressure cooled turbines continues to increase, there is an insistent need to explore many of the details of turbine fluid physics which have hitherto been overlooked, either because they seemed of second order or were simply too difficult to attack with the technical tools at hand. Three-dimensional effects on turbine flowfields fall perhaps in the first category while unsteady heat transfer and rotational effects may belong in the latter. Both of these problems could be studied at full scale in an engine, but that would be an extraordinarily complex task. The engine environment is extremely harsh, making instrumentation very difficult. The limited access to the turbine flow path exacerbates the problem as do the necessary safety and operational constraints which restrict parametric investigation. Also, of course, an engine is an expensive device to operate. One solution to the instrumentation access and parameter variation problem is a test facility designed for the full turbine environment. This can be even more expensive to build and operate, however (and as difficult to engineer), as a large development gas turbine engine.

There is also a need for lesser facilities which can simulate most of the important high pressure turbine parameters but in a more benign environment and at a much lower cost. The study of turbine fluid physics is, in particular, well suited to the use of transient facilities since most high speed turbine aerodynamics and heat transfer phenomena occur on blade passing time scales.

The goal of this project was to design, build, and utilize a short duration turbine test facility. The Blowdown Turbine Facility is designated to test 0.5 meter diameter, film cooled, high work turbines under rigorously scaled conditions. An integral part of this work has been the simultaneous development of the high frequency response instrumentation (aerodynamic and heat transfer) and the data acquisition system necessary to realize the facility potential.

Proper scaling of the turbine operating environment requires an understanding of the basic physical forces influencing fluid flow and heat transfer. Insofar as we know, it is the ratios of

forces and states which control fluid physics. Proper scaling for a rotating flowfield with heat transfer includes viscous forces (Reynolds No., $Re = \rho U D / \mu$), temperature ratios, rotational effects (Rossby No., $Ro = U / \Omega D$), thermal properties (Prandtl No., $Pr = C_p \mu / k$), compressibility (γ), and flow geometry (corrected speed and weight flow); where ρ is the fluid density, U the fluid velocity, D a characteristic length, μ the viscosity, Ω the rotational speed, C_p the specific heat at constant pressure, k the thermal conductivity, and γ the ratio of specific heats. Turbulence intensity may also have an important influence on the heat transfer. For a film-cooled turbine, the mass flux ratio ($\rho_c U_c / \rho_\infty U_\infty$) is of interest, where the subscripts c and ∞ refer to the coolant and the main flow. Facility scaling is illustrated in Table 1.

TABLE 1
MIT BLOWDOWN TURBINE SCALING

	Full Scale	MIT Blowdown
Fluid	Air	Argon/Freon-12
Ratio specific heats (γ)	1.27	1.27
Mean metal temperature	1118°K (1550°F)	295°K (72°F)
Metal/gas temperature ratio	0.63	0.63
Inlet total temperature	1780°K (2750°F)	478°K (400°F)
Cooling air temperature	790°K (960°F)	212°K (-77°F)
Airfoil cooling air	12.5%	12.5%
True NGV chord	8.0 cm	5.9 cm
Reynolds number*	2.7×10^6	2.7×10^6
Inlet total pressure, atm (psia)	19.6 (289)	4.3 (64)
Outlet total pressure, atm (psia)	4.5 (66)	1.0 (14.7)
Outlet total temperature	1280°K (1844°F)	343°K (160°F)
Prandtl number	0.752	0.755
Rotor speed, rpm	12,734	6,190
Mass flow, kg/sec	49.0	16.6
Power, watts	24,880,000	1,078,000
Test time	Continuous	0.2 sec

* Based on NGV chord and isentropic exit conditions.

There are many transient test facility configurations which could meet most if not all of the scaling criteria enunciated in the preceding section. Since the predominant source of unsteadiness in turbines is rotor-stator interaction, a test time on the order of 1,000 to 10,000 blade passings (0.1 to 1.0 seconds) should suffice for most studies.

The configuration selected (Figs. 1 and 2) consists of a supply tank separated by a large fast-acting valve from the test section containing the turbine stage which discharges into a vacuum dump tank. Prior to a test, the entire facility is evacuated (0.1 torr) by a mechanical vacuum pump. The supply tank and valve are then heated by oil circulating in a jacket around the tank. After the desired temperature is reached, the fast-acting valve is closed and the supply tank pressurized with the appropriate gas mixture. The turbine (which is still in vacuum) is brought to operating speed by a small electric motor. A direct coupled eddy current brake is used to absorb the turbine power and hence hold corrected speed constant. The test is initiated by simultaneously opening the valve and energizing the eddy current brake magnets.

The eddy current brake is attractive because the braking power is proportional to the square of the rotational speed while a choked turbine produces power as the square of the tip Mach number. Thus, an eddy brake coupled to the turbine matches the turbine characteristic without the need of a control system. Since the power absorption of the brake is also directly set by the magnet excitation current, a wide range of turbine powers can be readily accommodated. The eddy brake offered the advantage of a high power density design, simplifying packaging and rig layout. Unlike a mechanical friction brake, the eddy brake has no moving parts other than the conductor and thus relatively few mechanical and dynamic design problems.

The size of the downstream dump tank is set by the overall run time desired at a particular turbine pressure ratio. The supply tank size is set by the allowable change in temperature ratio during the test time (<1%). The coolant flow is fed from a supply tank separate from that for the main flow. Its size is set so that the volume ratio of the two supply tanks equals that of the flow rates. Thus, the blowing ratio across the film cooling holes is maintained constant over the test time.

The facility has been sized to allow testing at twice design Reynolds No. ($2 \times (3 \times 10^6)$) in argon-Freon or at design Reynolds No. in air, i.e. the facility design inlet total pressure is 10 atm, which corresponds to 40 atm at engine conditions. The maximum laboratory inlet total temperature is 533°K (500°F), thus facilitating carbon steel construction and the use of elastomer seals. This corresponds to a scaled engine temperature of 2300°K (3680°F), assuming a 1250°K (1790°F) metal temperature or 2500°K (4040°F) for a 1350°K (1970°F) metal temperature. Thus, the facility operating envelope includes the full range of present and proposed engine designs. Details of the facility design and construction can be found in Refs. [1] and [2].

4.1.1 Data Acquisition System and Instrumentation

The specification of the data acquisition system (DAS) was principally determined by the requirements for detailed examination of the time-resolved heat transfer and fluid flow in the high speed turbine. The 6 kHz blade passing frequency and relatively thin NGV wakes (1/5 to 1/10 of the blade spacing) dictated an analogous bandwidth of 30 to 100 kHz for each channel. The need for simultaneous heat transfer and pressure measurement along the airfoil surfaces required a large number of channels, 25 to 100. Thus, 5 to 20 million samples per second were required for the 0.1 to 0.4 second test time (considering sampling theorem restrictions), thus producing 1 to 8 million total samples.

The DAS was designed for 100 high speed, 12-bit channels with 200 kHz per channel maximum sampling rate. Up to 96 lower speed channels, organized into 8 groups of 16, were multiplexed onto 8 of the high speed channels. The high speed channels were used for the heat transfer gauges and high frequency pressure transducers which record the blade-to-blade flow, while the low speed channels were used for overall facility monitoring, pitot rakes, etc. The sampling rate was controlled by four programmable multispeed clocks (20 Hz to 200 Hz) which were individually set with a sampling rate and number of samples prior to a test. The data was stored in a 32 million byte solid state (RAM) memory for post-test readout to a host computer (DEC-PDP 11/70). The present configuration consists of 35 high speed channels, four 16-channel

multiplexers, and a 64-bit wide digital input stream. Twenty million data samples could be taken per test.

4.1.2 Flow Instrumentation

Most of the flow instrumentation in this facility was specially developed at MIT for the blowdown tunnel. It consisted of both time-averaging and time-resolved instrumentation including: traversing probes to measure total and static pressures and air angles, wall static transducers on the outer casing wall and NGV and rotor blade surfaces, and a total temperature-total pressure probe. Low frequency response pitot instrumentation was used where the flow was quasi-steady, as in the annulus upstream of the NGV's.

There were four probes which were used for radial and circumferential traversing behind the rotor or the NGV's with the rotor removed. The "four-way" probe consisted of four semiconductor strain gauge pressure transducers mounted around a 3 mm diameter cylinder. The transducers were arranged such that the probe can simultaneously measure total and static pressure and azimuthal and radial angles ($\pm 20^\circ$). Data reduction was done with the aid of calibrations performed as a function of Mach number. The probe was water cooled to increase thermal stability. Frequency response was determined by the cylinder size and rolls off above 12 kHz. The four-way probe was the only instrument small enough to traverse between the NGV's and the rotor, although interference and blockage effects were not determined.

Rotor outflow total temperature was surveyed using a dual hot wire aspirating probe which could simultaneously measure total temperature and pressure with a frequency response of dc to 20 kHz. The probe's dc accuracy was 1% while its resolution was 0.3%.

Wall static pressures were measured on the casing above the rotor and on the NGV and rotor blades with semiconductor transducers.

The steady test time of the facility was long enough to permit the use of carefully designed pneumatic instrumentation. This was used for comparison with similar measurements taken at Rolls-Royce Limited and as a lower cost scheme for measurements in regions of essentially steady

flow. These included conventional Kiel probes four chords downstream of the rotor exit and static taps around the NGV chord to record "tube averaged" airfoil static pressure distributions.

4.1.3 Heat Transfer Measurement

The total heat load in a turbine consists of both low and high frequency effects. The technique used to measure the surface heat flux in this rig therefore had to have sufficient bandwidth to observe both the "mean" and varying heat flux.

The primary instrumentation was thin film heat flux gauges distributed about the rotor blade profile. These transducers measured both the dc and ac components of heat flux. The heat flux gauges consisted of two thin film (140 nm thick) nickel temperature transducers mounted on either side of a 25- μ m-thick polyimide insulator. The sensing area was rectangular (1.0 x 1.3 mm), oriented such that the longer dimension was in the chordwise direction. The insulator was adhesively bonded to, and completely covered, the blade profile (preventing thermal discontinuities). At low frequencies, the temperature drop across the insulator was a direct measure of the heat flux to the wall (the device is essentially a thermal shunt). This direct proportionality between heat flux and temperature difference extended from dc to about 20 Hz, at which point the thermal waves within the insulator began to damp. Above 1 kHz, however, the 25- μ m-thick insulator appears infinitely thick to the top surface. Thus, above this frequency, a quasi-one-dimensional assumption could be used to infer the heat flux from the top surface temperature history (blade passing frequency is 6 kHz). Using a numerical data reduction technique, the entire frequency domain from dc to 100 kHz was reconstructed. The gauges were calibrated using a pulsed laser. The relative gauge calibrations were accurate to better than 5 percent. Absolute calibration accuracy was about 10 percent. Details of the gauge theory, data reduction, and calibration may be found in Ref. [3]. This heat flux gauge was invented and patented under this contract.

4.1.4 Optical Flow Diagnostics

Part of this work included an attempt to develop optical flow diagnostics suitable for high

speed turbine geometries and flowfields using laser induced fluorescence (LIF) of 2,3 butanedione, a gas mixed with the flow. In particular, it was hoped that through comparison of the simultaneous emission of the singlet (blue) and triplet (green) states, static gas temperature could be measured. The ratio of blue to green emissions did prove to be sensitive to temperature. However, the relatively long life of the triplet state (tens of microseconds) rendered the technique inappropriate in an unsteady, transonic flowfield in which all measurements must be made in 1–2 μ s. The technique is quite viable for lower speed flows, however. More details may be found in Ref. [4].

4.1.5 Facility Performance

The facility and instrumentation proved to work quite well. All corrected turbine flow parameters could be kept constant to better than 1/2% for more than 300 ms, sufficient time for all aerodynamic and heat transfer measurements to be made.

4.2 Experimental Measurements

Experimental measurements of the flow quantities listed in Table 2 were made under a variety of flow conditions, varying gas to wall temperature ratio, rotor corrected speed (rotor incidence angle), Reynolds number, and turbine pressure ratio. Several key findings were made. The first was that the heat transfer to the turbine rotor and tip shroud is truly unsteady with fluctuations typically of $\pm 100\%$ of the mean value. Examples are given in Fig. 3 for the endwall and Fig. 4 for the rotor. The implication is that models treating the flow and heat transfer process as steady are liable to be inaccurate since the unsteady flow physics are not included.

The second important experimental conclusion is that the heat transfer at turbine rotor blade midspan is extremely similar to that made on a stationary cascade with unsteady inflow generated by rotating bars (Fig. 5). Thus, at least for the midspan of the turbine studied, the principal "real turbine" effects are those of unsteadiness, not rotation.

TABLE 2
FLOW QUANTITIES MEASURED IN FACILITY

	Steady	Time-Resolved
1. Heat Transfer		
Rotor	✓	✓
Nozzle	✓	✓
Rotor Tip	✓	✓
2. Total Pressure		
Stage Inlet	✓	
Rotor Relative Inflow	✓	✓
Rotor Outflow	✓	✓
3. Total Temperature		
Stage Inlet	✓	
Rotor Outlet	✓	✓
4. Turbulence Intensity		
Stage Inlet		✓
5. Wall Static Pressure		
Nozzle	✓	✓
Rotor Blade	✓	✓
Rotor Tip Shroud	✓	✓
6. Flow Angle		
Rotor Exit	✓	✓
7. Freestream Static Pressure		
Rotor Outlet	✓	✓
8. Torque and RPM	✓	

The third conclusion from the measurements is that the turbine rotor tip shroud heat transfer decreases moving along the shroud from upstream to downstream. This decrease is readily explained by the decrease in enthalpy of the flow relative to the stationary shroud due to the work extraction by the rotor. Thus, the decrease of the driving temperature is mainly responsible rather than large changes in the heat transfer coefficient. This finding is somewhat at odds with engine experience in which it is the aft section of the shroud which suffers the most thermal distress. This may be due to a cooling effect or due to the influence of the temperature nonuniformities

characteristic of combustor exit flows which were not simulated in this experiment.

As with the heat transfer, the aerodynamics of the turbine were found to be highly unsteady. This can be seen in Fig. 6 of the rotor relative total pressure, and in Fig. 7 of the rotor exit Mach number distribution measured with high frequency response instrumentation.

5.0 COMPUTATIONAL EFFORT

The computational effort was aimed at the development of steady, two- and three-dimensional viscous, and two-dimensional multiblade row unsteady computer codes for the calculation of the flow and heat transfer in transonic turbines. A key feature of the effort was to develop codes which were accurate at reasonable run times on large computers so that they would be of use as practical engineering tools. The codes were developed on computers equipped with array processors. The principal objective of the activity was not the production of computer codes but rather the creation of research tools and the use of those tools, in conjunction with the experimental measurements, to elucidate the fluid mechanics and heat transfer in high pressure turbine stages. Efforts included the development of new solvers, boundary conditions, and grid generators, the details of which may be found in the references. Here we will describe only the integrated codes.

The research on the computational side of the project falls naturally into two parts, with the first being the development of two-dimensional and three-dimensional methods for calculating steady, viscous flows, and the second being spent on developing a new approach for unsteady flow calculations.

The principal accomplishment of the first effort was the development of a numerical method for solving the steady, Reynolds-averaged Navier-Stokes equations in a rotating coordinate system. The rotational effects required the inclusion of Coriolis and centrifugal forces. Turbulent flows were handled by the use of a relatively simple algebraic turbulence model. Using this method, we performed the first calculation of the viscous flow past a rotating turbine. The results show the radial movement of boundary layer fluid on the rotor, and the formation of a strong vortex at the hub/rotor junction in which fluid moves upstream under the influence of a local adverse pressure gradient, which in turn is caused by a sharp flare in the hub geometry. These are typical of the kind of important flow structures which can only be calculated with a fully three-dimensional method, and illustrate the capability of computational techniques to capture the details of fundamental physical processes which are difficult to investigate experimentally.

To aid in the development of the three-dimensional code, a two-dimensional version was also written. Although this program was intended only for steady-state calculations, it is also capable of calculating unsteady flows, although rather inefficiently. Consequently, in support of the experimental work in this project (but using funding from another related project), we used the program to calculate the unsteady flow in the compressor which was being investigated experimentally. The calculation revealed a number of interesting features. Firstly, it confirmed the existence of vortex shedding at the trailing edge of the compressor, and the shedding frequency was in good agreement with the experimental data obtained using a number of different methods. It also showed rather well that the shedding on the suction surface is due to a roll-up of the vorticity in the suction surface boundary layer and so the relevant length scale in determining the correct Strouhal shedding frequency is the boundary layer thickness, or equivalently the wake thickness, not the trailing edge radius as used for shedding from cylinders and turbines. The second, unexpected feature was a low frequency oscillation in the shedding frequency and strength which was due to an oscillation in the suction boundary layer thickness, which in turn was due to a motion in the separation point. There was also a slight shock motion but it was not clear whether this was a cause or an effect. The engineering significance of this oscillation lies in the fact that it occurs at a frequency close to the primary structural frequencies and so could cause catastrophic failures. The presence of this low frequency oscillation is supported by some experimental observations, which on their own would not have been particularly convincing. This illustrates one of the basic premises of this research project, that the combination of experimental and computational research (each with their own inherent uncertainties and weaknesses) is much more powerful than either alone.

One problem in performing the compressor calculation was that one calculation, comprising many vortex shedding periods but only a few of the low frequency oscillations, required over two months of CPU time on our computer. This prevented us from doing a systematic investigation of the dependence of the phenomena on various parameters. To be able to do this in the future requires a fresh start and the development of a numerical method for efficient, accurate calculations

of unsteady flow. This research development began in the last year of the current project. There will be several steps in the development process towards the ultimate goal of calculating the unsteady, viscous flow caused by the interaction of a closely spaced rotor and stator, including such details as the unsteady vortex shedding and the unsteady pressure waves which give rise to undesirable increases in losses, vibration and noise. The program which has been developed at present calculates the unsteady inviscid flow in a rotor row subject to unsteady boundary conditions corresponding to incoming, viscous wakes and isentropic pressure disturbances from a neighboring stator row. One of the key algorithm developments is the ability to analyze cases in which the rotor blade pitch is different from the stator pitch. This was achieved by the novel method of "inclining" the computational plane, meaning that the computational plane at one "time-level" no longer corresponds to one physical time. This is necessary to implement the lagged periodic boundary condition that arises in cases with unequal pitches. The full details are available in the referenced reports. Results for a number of test cases (including simple flat plate cascade model problems) are in agreement with experimental, computational and theoretical work by other researchers. In practical applications, the results show the deformation of the wake due to the faster flow in the middle of the blade passage, the cutting of the wake by the rotor, and the subsequent generation of a pair of counter-rotating vortices formed by the rolling up of the positive and negative vorticity in the wake segments. As well as affecting heat transfer and generating noise, the unsteady fluctuations cause a variation of 3% or more in the lift and moment which are large enough to be very significant.

6.0 COMPARISON OF CALCULATIONS AND EXPERIMENT

The two-dimensional steady and unsteady codes were used to predict the time-averaged and time-resolved heat transfer and static pressure distributions about the rotor midspan and compared to measurements from the blowdown turbine and from a cascade. Examples are given below.

Predictions from the two-dimensional version of the steady three-dimensional code, ANSI, were made for the design point operating conditions of the turbine geometry in the blowdown turbine. The grid (Fig. 8) used was of the type described by Norton et al. [5] and employed an O-type grid about the blade for ready calculation of the eddy viscosity in the boundary layer (since the mesh is normal to the blade surface). The O grid is embedded in a C-type grid used to enhance resolution in the blade wake. The C grid is in turn embedded in an H grid used for the throughflow calculation. Near the leading edge, the O grid resolution is low in the streamwise direction, resulting in elongated cells in the boundary layer near the stagnation point. The grid resolution normal to the blade surface for the O, C, and H grids is 5, 11, and 16 nodes, respectively. A total of 5100 cells was used.

For the calculations presented here, the inflow conditions and wall temperature were matched to those of the experiment. The code has no empirical, adjustable "knobs" other than the transition location. Transition was specified as a point near the leading edge of the airfoil ($x/s = 0.01$).

As can be seen in Fig. 9, except for near the leading edge, the rotor measurements agree quite well with the fully turbulent two-dimensional prediction. A dip in heat transfer at about 80 percent surface distance on the suction surface, evident in both the measurements and calculations, is seen in the calculation as due to the impingement of the oblique expansion wave from the trailing edge of the adjacent blade. The large spike in the calculated heat flux at the trailing edge is an artifact of the lightly damped steady solution of what is physically an unsteady flowfield. Time-accurate solutions of this airfoil show vortex shedding at the trailing edge. The pronounced downspike near the leading edge in the calculation results from the greatly elongated cells used in this region of the boundary layer and the spatial first-order accuracy of the boundary conditions at

the wall combining to limit accuracy in this area.

Data taken from cascade tests at the University of Oxford (Fig. 10b of Ashworth et al., 1985) on the same profile shape (at larger physical scale) at similar conditions is also presented. The cascade data plotted are those with low freestream turbulence (0.8 percent) and bar passing generated disturbances (shock waves and wakes) upstream of the blade row. Because the Reynolds number of the rotor test was about 15 percent lower than that for the cascade, the cascade data are plotted both as presented in Ashworth et al. and scaled by the Reynolds number ratio to the 0.8 power. (This scaling is shown without necessarily endorsing a 0.8 power relation.) Overall, the agreement between an *ab initio* two-dimensional calculation, two-dimensional cascade tests, and full-stage tests is quite close.

The unsteady, multiblade row code, UNSFLO, was also compared to data. In steady state mode, it does a very good job of predicting the pressure distribution about the blade, Fig. 10, as well as the heat flux distribution. Time accurate heat flux predictions corresponding to suction surface and pressure surface gauge locations (3 and 9 in Fig. 4) show quite good agreement. The peaks in Fig. 11 are caused by interactions of the upstream blade row shock wave system with the rotor blade. The wake interaction with the boundary layer (Fig. 12) is not accurately modelled by the algebraic turbulence model in the code.

Overall, UNSFLO gives excellent agreement with the experimental data.

7.0 CONCLUSIONS

We have built a new type of experimental apparatus (including the necessary instrumentation) and written viscous steady and unsteady computational fluid mechanics codes in order to study the fluid mechanics and heat transfer in high pressure turbine stages. The results show that the heat transfer and fluid mechanics processes in these machines are mainly unsteady. The flow is explained in terms of the unsteady mean, shock wave, and wake flow interactions between the blade row. The codes do quite a good job of predicting the necessarily spatially sparse experimental measurements. The greater resolution of the computational representation was extremely useful in interpreting the measurements and understanding the flowfield. This is clearly a case of the whole being greater than the sum of the parts.

Aside from the scientific findings, the techniques developed as part of this effort have proved useful in and of themselves. The thin film heat flux gauge instrumentation is being adopted by a variety of experimenters. The blowdown turbine is being duplicated in large scale by the USAF for routine testing of advanced military turbines. The CFD codes have been distributed to a number of industrial, government, and university groups. Some of the codes are routinely used for the design of advanced aircraft gas turbine engines.

Perhaps the most interesting technical conclusion from this work is a negative one. One of the original goals of this project was to explain the empirically observed difference between simple cascade flows and those in full scale engines. We were frankly surprised by the results reported herein which showed that rotating, three-dimensional blade row interactions -- done at full Reynolds number, Mach number, etc. -- do not explain this difference. These results match those of the cascade quite closely, not those of the engine. The implication is that phenomena not modelled in facility or computer codes are responsible for this difference. The only candidates we can identify are turbulent intensity level and turbine inflow inhomogeneities (mainly combustor pattern factor). Only further work in this area can answer this question.

8.0 REFERENCES

1. Epstein, A.H., Guenette, G.R., Norton, R.J.G., "The MIT Blowdown Turbine Facility," ASME Paper No. 84-GT-116, 1984.
2. Epstein, A.H., Guenette, G.R., Norton, R.J.G., "The Design of the MIT Blowdown Turbine Facility," MIT Gas Turbine Laboratory Report No. 183, April 1985.
3. Epstein, A.H., Guenette, G.R., Norton, R.J.G., Yuzhang, C., "High Frequency Response Heat Flux Gauge," *Review of Scientific Instruments*, Vol. 57, No. 4, 1986, pp. 639-649.
4. Lewis, M.J., "Fluorescent Gas Measurements of Static Temperature and Density in a Turbine Stage," S.M. Thesis, MIT Department of Aeronautics and Astronautics, May 1985.
5. Norton, R.J.G., Thompkins, W.T., Jr., Haimes, R., "Implicit Finite Difference Schemes With Non-Simply Connected Grids--A Novel Approach," AIAA Paper No. 84-0003, 1984.

9.0 PUBLICATIONS AND REPORTS UNDER THIS EFFORT

Bush, R.H., "Prediction of Complex, Viscous, Compressible, Internal Flow Using Implicit Finite Difference Methods," MIT Gas Turbine Laboratory Report No. 175, October 1983.

Epstein, A.H., Guenette, G.R., Norton, R.J.G., "The MIT Blowdown Turbine Facility," ASME Paper No. 84-GT-116, 1984.

Norton, R.J.G., Thompkins, W.T., Jr., Haimes, R., "Implicit Finite Difference Schemes With Non-Simply Connected Grids--A Novel Approach," AIAA Paper No. 84-0003, 1984.

Epstein, A.H., Guenette, G.R., Norton, R.J.G., "The Design of the MIT Blowdown Turbine Facility," MIT Gas Turbine Laboratory Report No. 183, April 1985.

Holt, J.L., "Time Resolved Flowfield Measurements in a Turbine Stage," M.S. Thesis, MIT Department of Aeronautics and Astronautics, May 1985.

Lewis, M.J., "Fluorescent Gas Measurements of Static Temperature and Density in a Turbine Stage," S.M. Thesis, MIT Department of Aeronautics and Astronautics, May 1985.

Epstein, A.H., Guenette, G.R., Norton, R.J.G., Yuzhang, C., "High Frequency Response Heat Flux Gauge for Metal Blading," Invited Paper, AGARD 65th PEP Symposium, Norway, May 1985.

Epstein, A.H., et al., "Time Resolved Measurements of Turbine Rotor Stationary Tip Casing Pressure and Heat Transfer Field," AIAA Paper 85-1220, presented at AIAA Joint Propulsion Conference, Monterey, CA, July 1985.

Zaretsky, B., "The Prediction of Transition Region in Boundary Layers," S.M. Thesis, MIT Department of Aeronautics and Astronautics, July 1985.

Guenette, G.R., "A Fully Scaled Short Duration Turbine Experiment," Ph.D. Thesis, MIT Department of Aeronautics and Astronautics, August 1985.

Epstein, A.H., Guenette, G.R., Norton, R.J.G., Yuzhang, C., "High Frequency Response Heat Flux Gauge," *Review of Scientific Instruments*, Vol. 57, No. 4, 1986, pp. 639-649.

Epstein, A.H., "Short Duration Testing for Turbomachinery Research and Development," keynote paper for the Second Symposium on Transport Phenomena, Dynamics, and Design of Rotating Machinery, Honolulu, HI, April 1988.

Guenette, G.R., Epstein, A.H., Haimes, R., Giles, M.B., "Fully Scaled Transonic Turbine Rotor Heat Transfer Measurements," ASME paper 88-GT-171, presented at the 33rd ASME Gas Turbine Conference, Amsterdam, June 1988.

Giles, M.B., "Stator/Rotor Interaction in a Transonic Turbine," AIAA Paper AIAA-88-3093, presented at the AIAA/SAE/ASME/ASEE 24th Joint Propulsion Conference, Boston, MA, July 1988.

Giles, M.B., "Calculation of Unsteady Wake/Rotor Interaction," *AIAA Journal of Propulsion and Power*, Vol. 4, No. 4, July-August 1988, pp. 356-362.

Guenette, G.R., Epstein, A.H., Haimes, R., Giles, M.B., "Fully Scaled Transonic Turbine Rotor Heat Transfer Measurements," *J. of Turbomachinery*, Vol. 111, Jan. 1989, pp. 1-7.

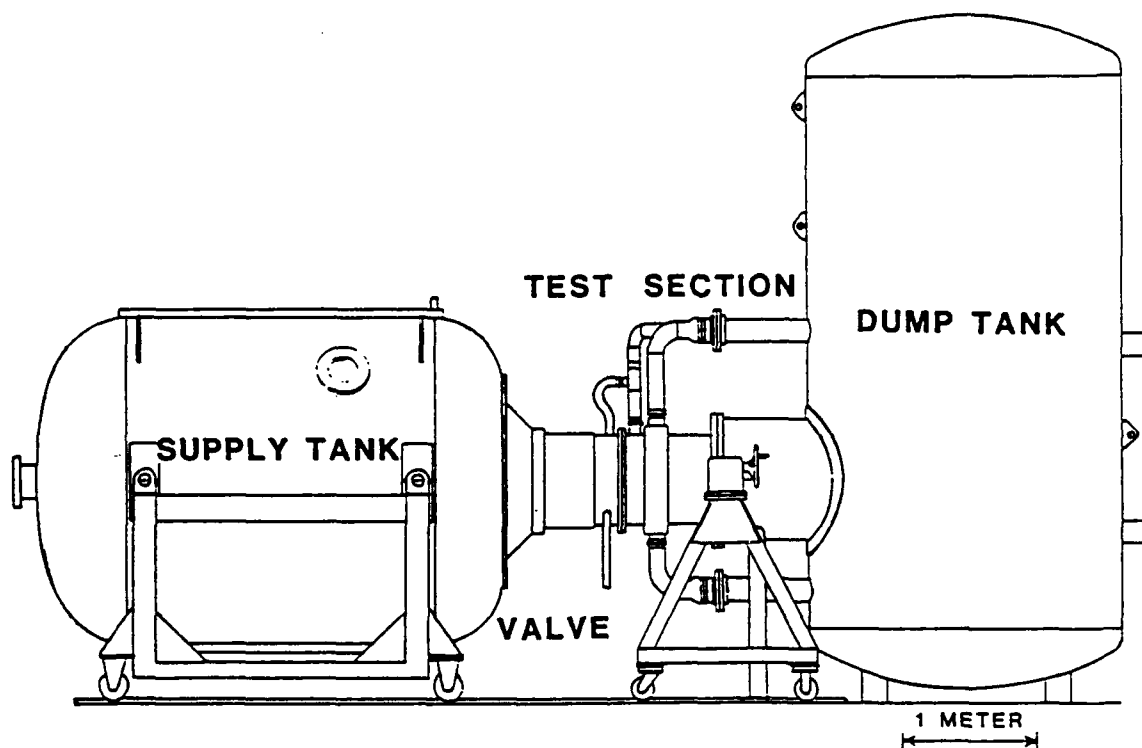


Fig. 1: Blowdown turbine facility outline

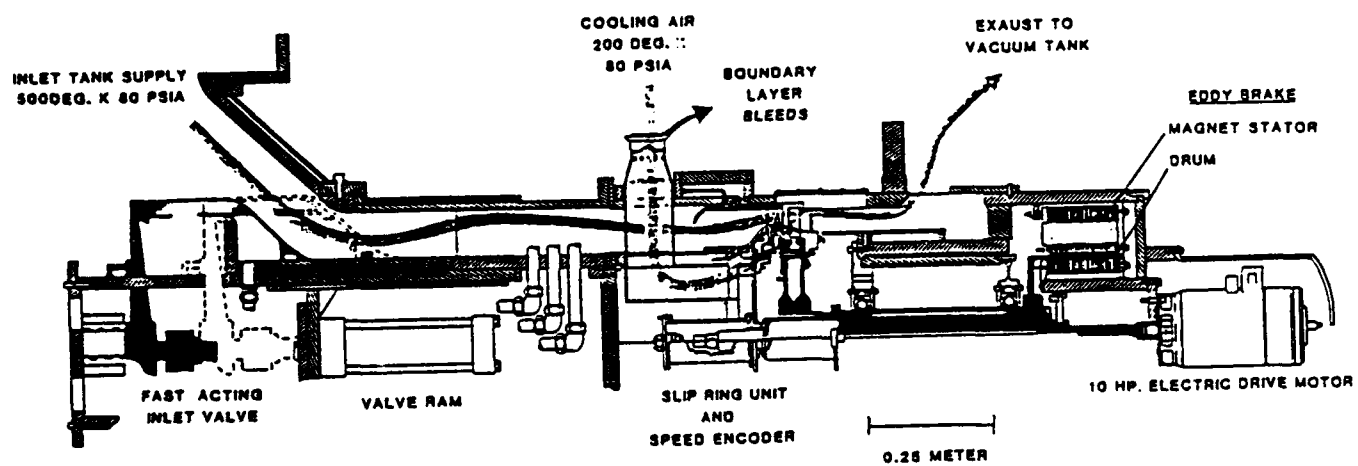


Fig. 2: Turbine facility flowpath

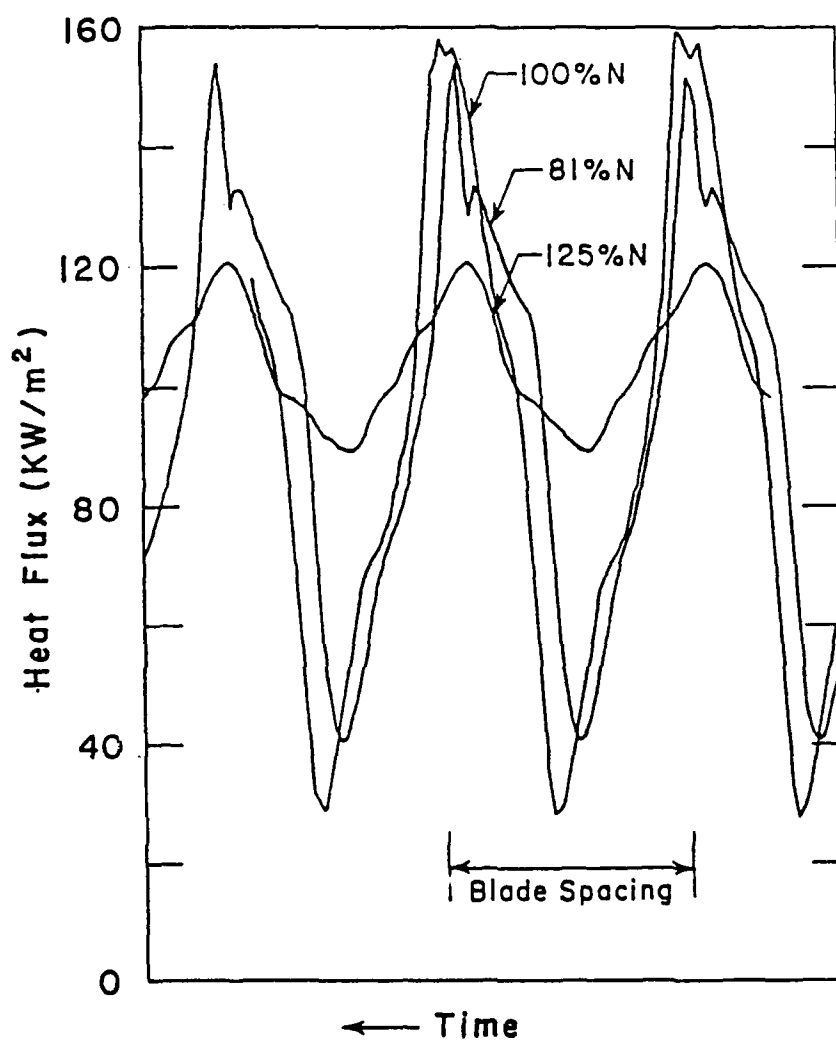


Fig. 3: Time-resolved heat transfer to stationary rotor tip casing near midchord at three different rotor speeds

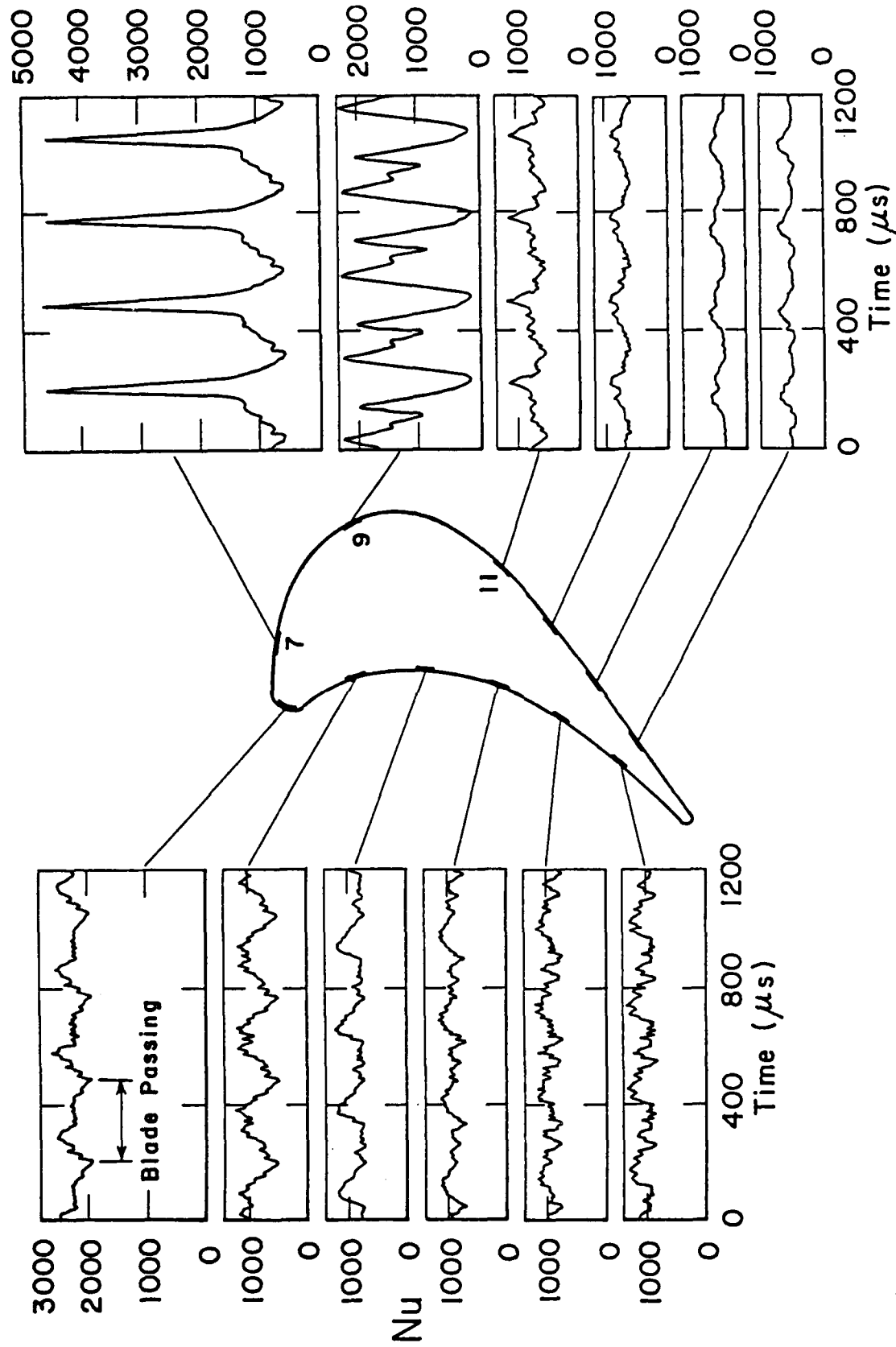


Fig. 4: Ensemble average of time-resolved heat flux measurements about the rotor blade midspan

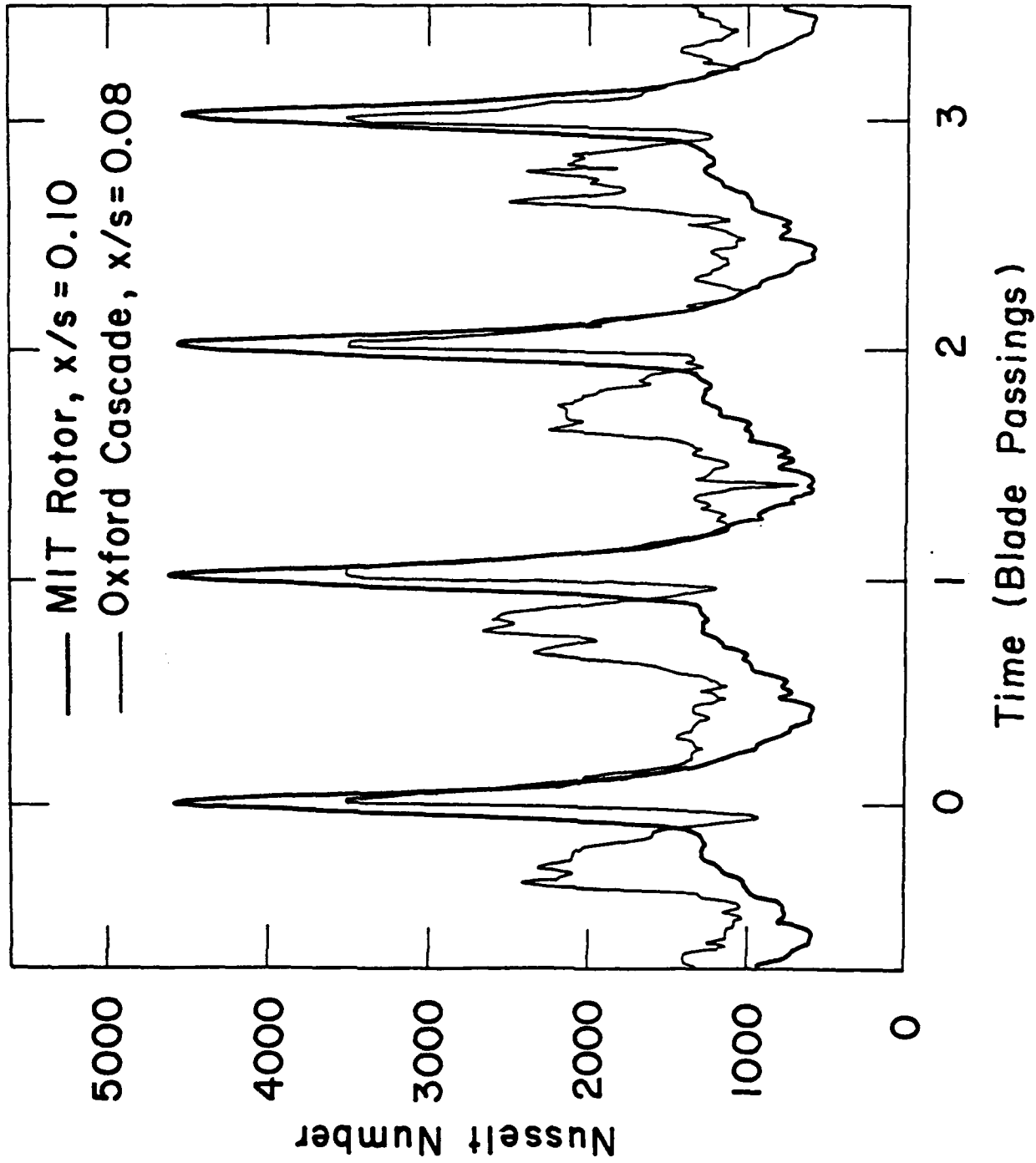


Fig. 5: Turbine rotor suction surface heat transfer history compared to that for the same blade shape in a two-dimensional cascade with upstream rotating bars

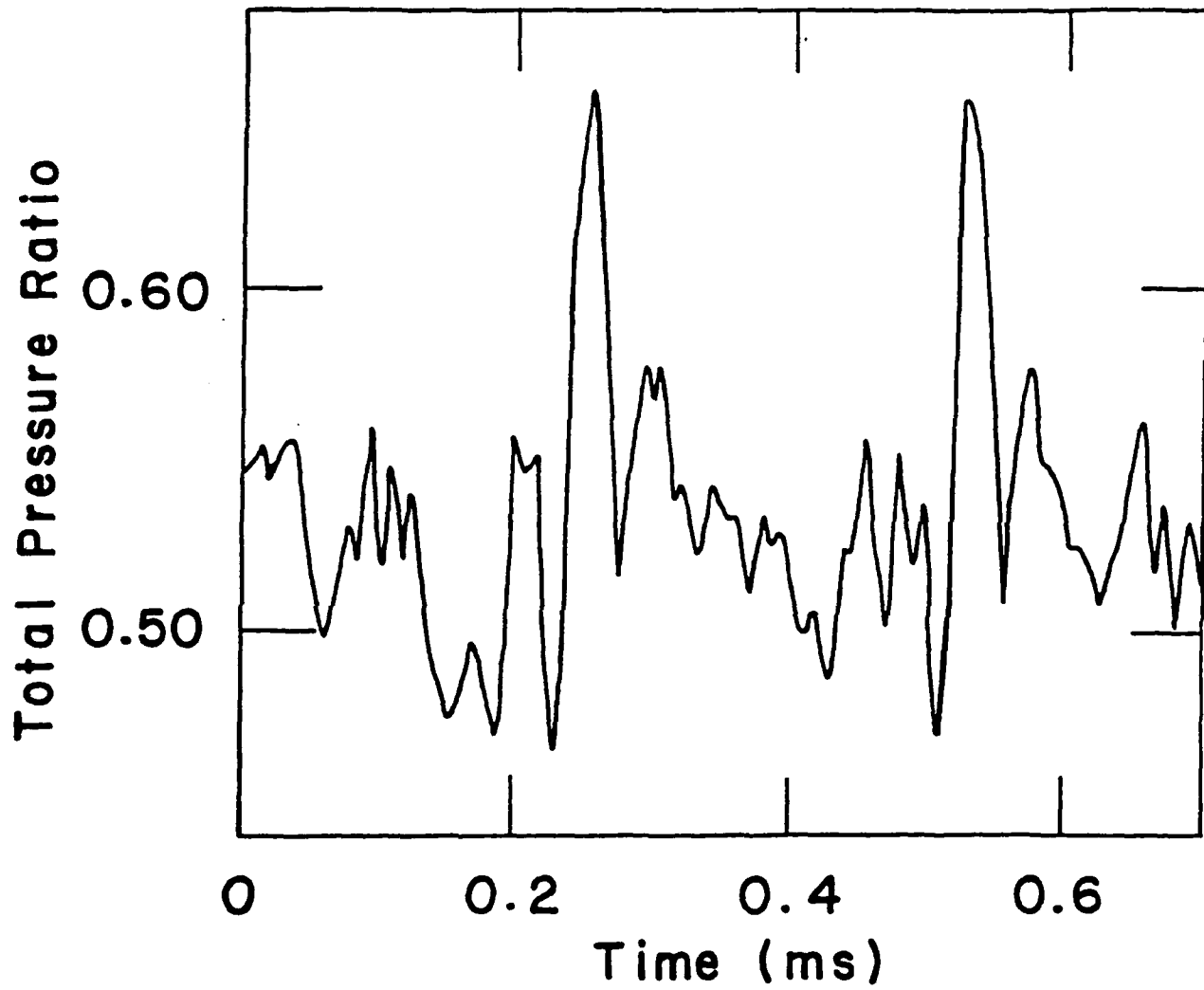


Fig. 6: Time-resolved rotor inlet total pressure measured with a probe cantilevered off the rotor leading edge at midspan

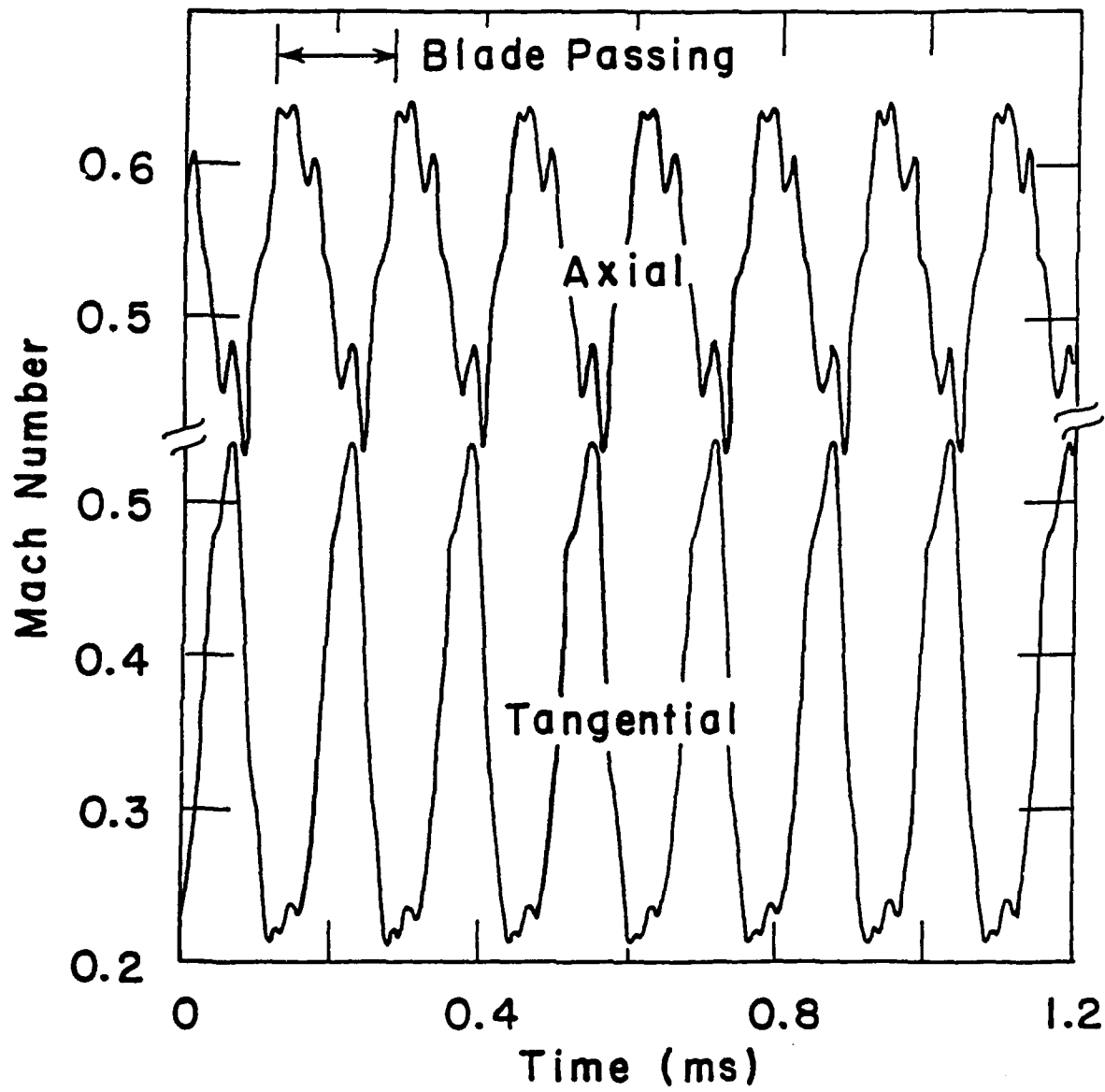


Fig. 7: Time-resolved rotor exit Mach number

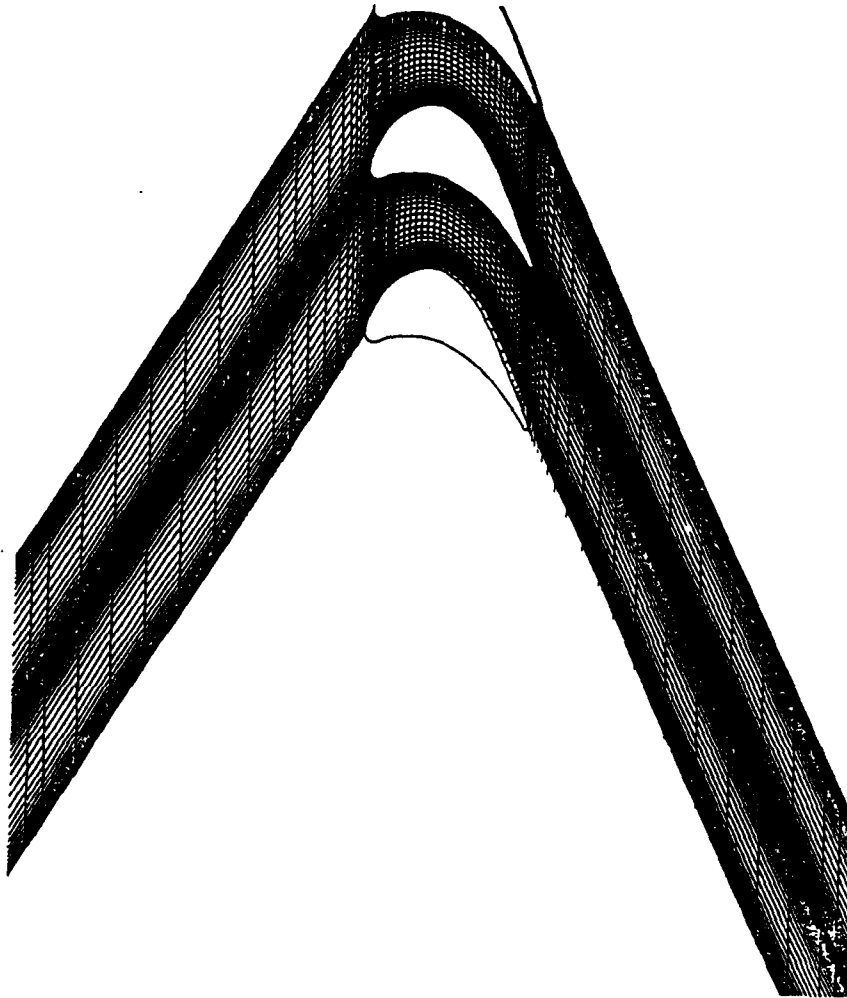


Fig. 8: Grid used for two-dimensional viscous calculation

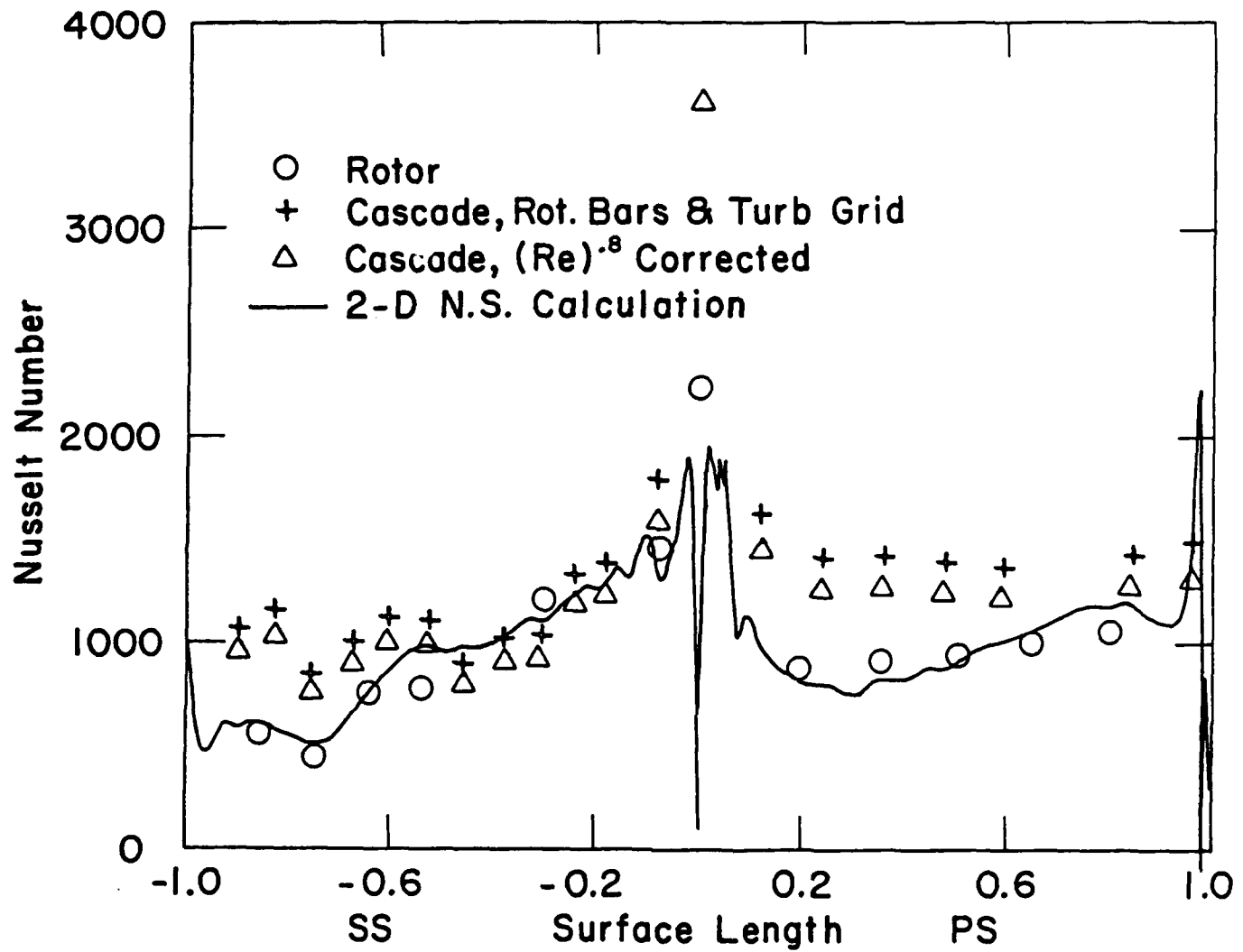


Fig. 9: Comparison of time-averaged experimental and steady state calculated heat transfer about the turbine rotor blade at midspan

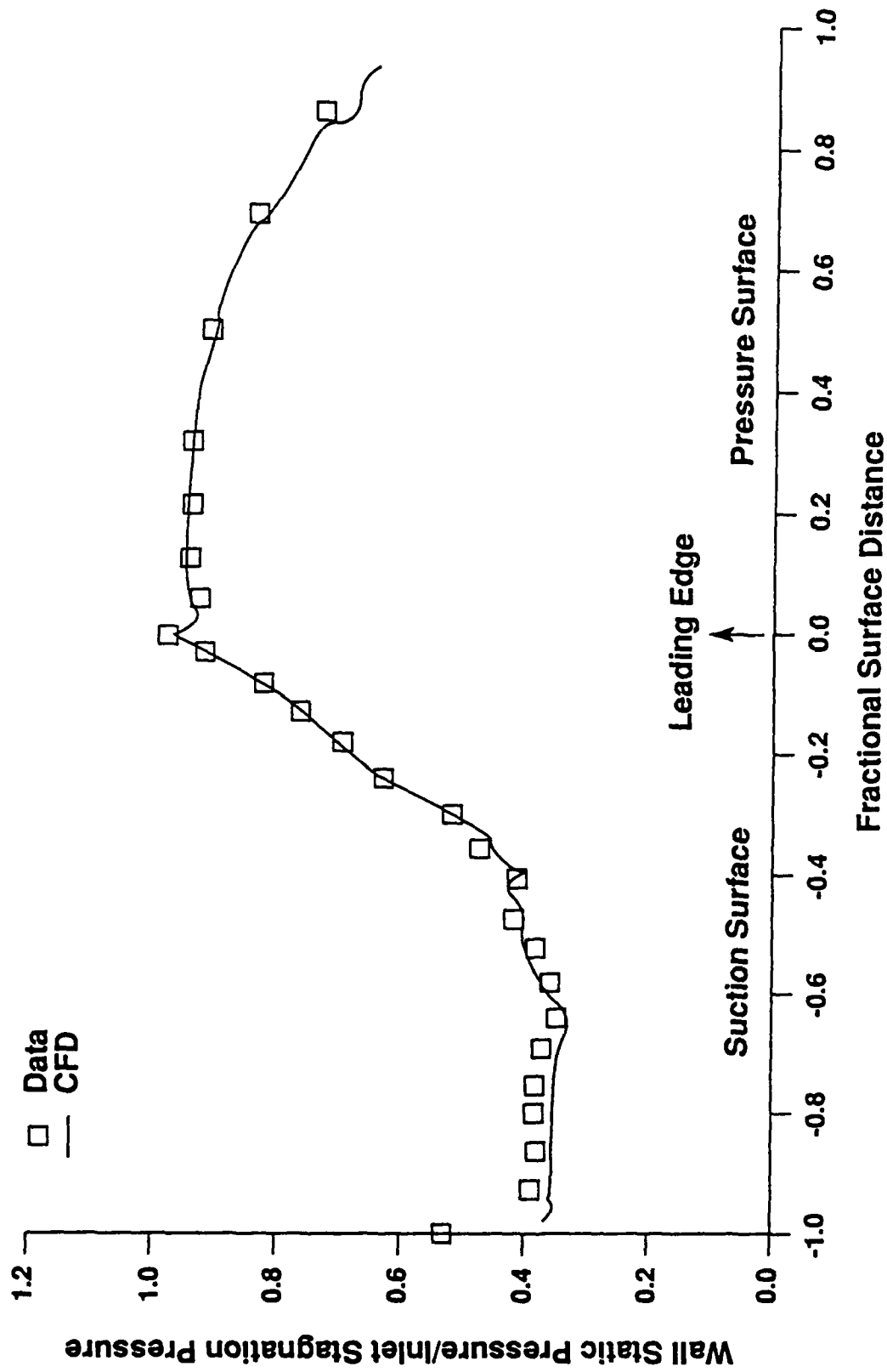


Fig. 10: Comparison of measured and calculated static pressure distribution about the rotor blade midspan profile in a cascade

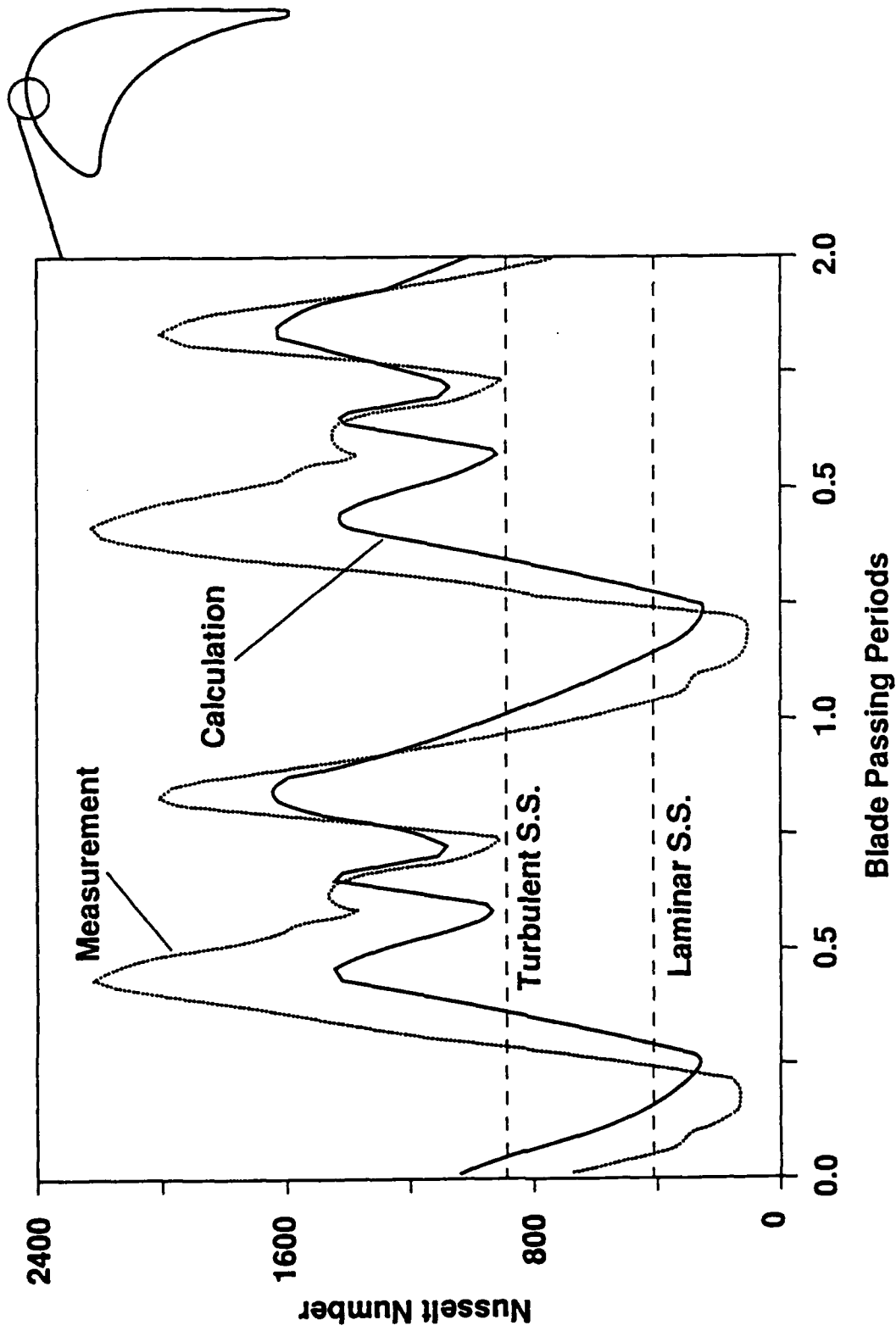


Fig. 11: Comparison of measurement and UNSFLO CFD code prediction of time-resolved heat transfer at rotor blade midspan on the suction surface

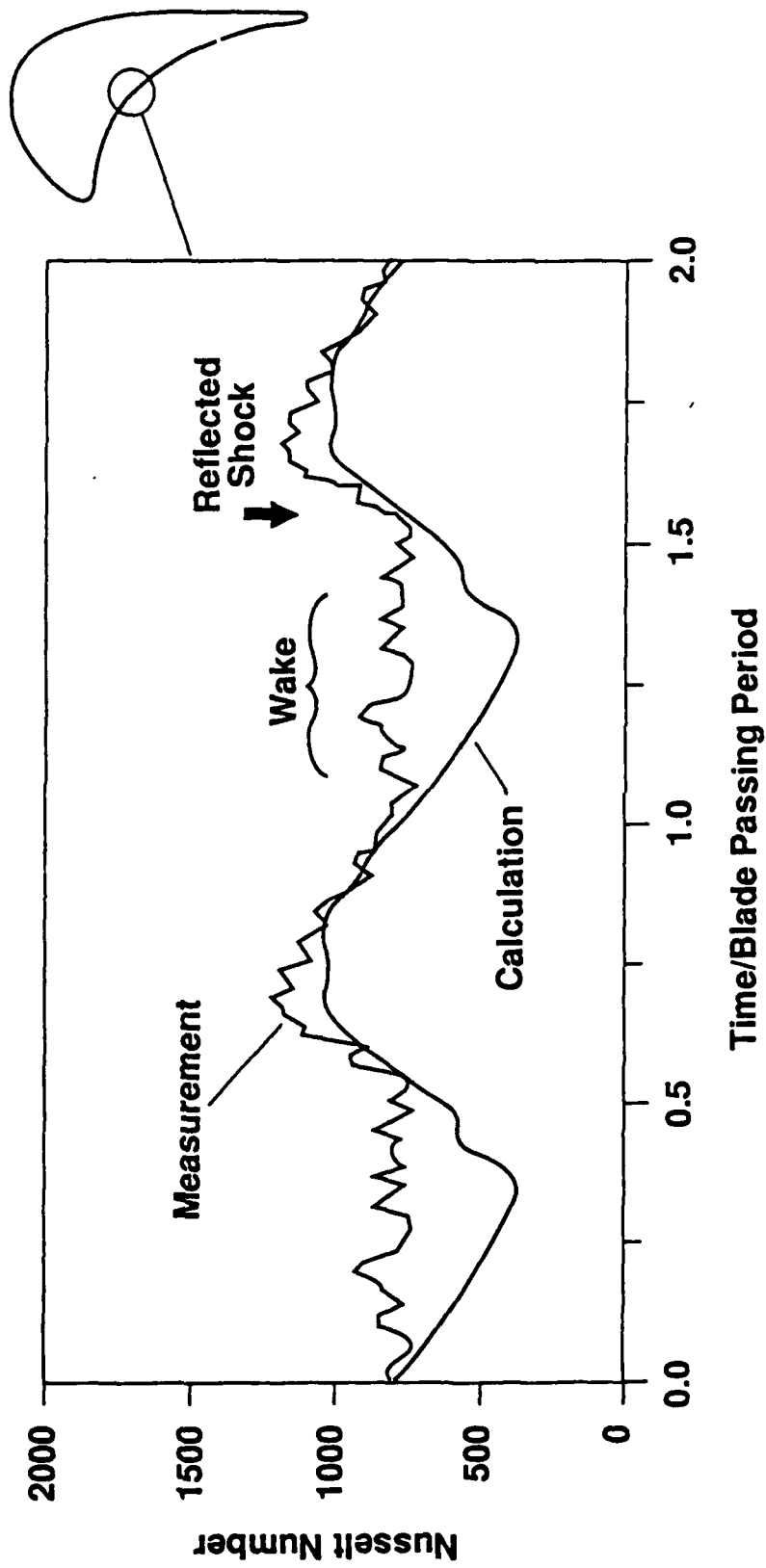


Fig. 12: Comparison of measurement and UNSFLO CFD code prediction of time-resolved heat transfer at rotor blade midspan on the pressure surface